Harvesting MDT Data: Radio Environment Maps for Coverage Analysis in Cellular Networks

Ana Galindo-Serrano, Berna Sayrac
and Sana Ben Jemaa
Orange Labs., 38-40 rue du Général Leclerc, 92794
Issy les Moulineaux cédex 9, Issy-Les-Moulineaux, France.
E-mail: anamaria.galindoserrano@orange.com

Janne Riihijärvi and Petri Mähönen
Institute for Networked Systems
RWTH Aachen University, Aachen, Germany

***Abstract*—Despite the remarkable progress in radio access technology to support the rapidly increasing wireless data demand, coverage analysis remains as one of the indispensable topics on which mobile operators still need innovations, above all, in terms of operational efficiency together with performance. Manual coverage detection and prediction is an inefficient and costly task. In this paper we show how Radio Environment Maps (REMs) developed as part of the research on cognitive wireless networks can be used as a basis for a powerful coverage estimation and prediction solution for present-day cellular networks. Applying powerful spatial interpolation techniques on the information coming from location-aware devices, REMs provide a realistic and remote representation of the ground-truth. The proposed approach automatically identifies the number, location and shape of the existing coverage holes and therefore constitutes a perfect example of a novel application of the Cognitive Radio concept on next generation cellular networks. Results on urban and rural environments show that the use of REM brings promising gains in coverage hole detection and prediction with respect to the case where only measurements are used.**

***Keywords*—Coverage hole detection, minimization of drive tests, spatial information exploitation, REM.**

I. Introduction

One of the most crucial and complex tasks when deploying a Radio Access Technology (RAT), is coverage planning. Despite a very careful coverage planning during the deployment phase, the existence of coverage holes during the operational phase is a common and almost unavoidable problem that operators need to address with high priority. For this purpose, first, it is necessary to detect the coverage holes (a process called as *coverage hole detection*), and then deploy a solution which remedies/removes the coverage problem in the uncovered zones. The deployed solution must be cost-efficient and well-performing. In order to achieve such a solution, we need the precise information on the location and shape of the coverage holes. Obtaining this information is called as *coverage hole prediction*. Obviously, the effectiveness of the deployed solution, highly depends on the performance of the detection and the prediction.

The focus of this paper is coverage hole detection and prediction. We show that methods originally developed for interference management in the context of cognitive wireless networks can be used very effectively for dealing with coverage holes in cellular networks. Further, we argue that these automated cognitive techniques offer significant benefits over the current approaches, which rely heavily on human interaction. The traditional way to deal with the coverage estimation task is to: (1) perform *drive tests*, which consist of collecting geo-located measurements of different metrics/indicators with a motor vehicle equipped with specialized mobile radio measurement equipments and Global Positioning System (GPS), and to (2) analyze the collected measurements for coverage hole detection and prediction. This analysis is performed manually by human experts. Drive tests are inefficient and very expensive solutions but they allow the operators to have realistic information on the "ground-truth". Therefore, it is mandatory for the operators to make the most of the information collected through drive tests, and to minimize the use of them. To this end, the cellular network-related standardization body, the 3rd Generation Partnership Project (3GPP), has included a feature on Minimization of Drive Tests (MDT) since Release 9 [1]. Due to the cost reduction promised by MDT, it is seen as one of the highest-priority features of next generation cellular networks, and therefore a considerable amount of effort is put forward for its standardization, product development and marketing.

The basic concept of MDT is that the User Equipments (UEs) report their geo-located measurements to the network upon operator request. The main difference between traditional UE measurement reporting and MDT is twofold: (1) the geo-location information of MDT is based on the GPS technologies available in mobile devices whereas the geo-location information of traditional UE measurements are at the cell level; (2) MDT measurements are collected and stored in a data repository called Trace Collection Entity (TCE) at the operator's Operation and Management Center (OMC) [2], hence allowing the operator to have direct access on the measurements, whereas the traditional UE measurements are processed by the base stations for Radio Resource Management (RRM) purposes and are inaccessible to the operator at the OMC level. The collected MDT measurements are at operator's direct disposition to ease any kind of (automated as well as manual) network operation, management and optimization task.

Geo-location information calls for the concept of *location/environment awareness* put forward by Mitola in the context of Cognitive Radio [3]. Inspired by this connection, a cognitive tool called as *Radio Environment Maps (REMs)* has been introduced and developed for diverse wireless network operation, management and optimization tasks. The concept of REM was first introduced in [4] where it has been presented as an integrated database, mainly for opportunistic/hierarchical/dynamic spectrum access purposes (i.e. TV

CROWNCOM 2013, July 08-10, Washington DC, United States

DOI 10.4108/icst.crowncom.2013.252055

whitespaces). The REM stores geo-location information, radio measurements, environmental information and past experience. Shortly after, a more comprehensive/cognitive version of REMs, also called as *Interference Cartography (IC)*, has been proposed for a mesh-like REM structure where the location points are found on a rectangular grid (i.e. the *pixels*). In this type of REM, the main idea is to: (1) *spatially interpolate* the collected geo-located measurements in order to predict the measurement values at those pixels where the operator does not have measurements, and to (2) request additional measurements at intelligently chosen pixels to enhance the quality of those predictions [5]–[7]. This paper falls in this latter line of work and unless otherwise stated, REM will mean IC.

As can be noticed easily, the IC concept fits perfectly into both the MDT and the Cognitive Radio framework. While the MDT measurements provide the exact input needed for constructing the REM, the REM brings environment awareness to today's cellular networks as a step forward for tomorrow's "cognitive cellular networks". Although the notion of REM also contains a *temporal* component, i.e. dynamic REMs, where the REM is updated iteratively with new measurements, here we consider a semi-static REM which represents the snapshot of an environment which changes slowly. Since our focus is particularly on outdoor coverage scenarios in urban and rural areas, which changes quite slowly (typically in the order of days to months), the choice of semi-static REMs is justified.

In this paper, we expand our previous work [8], which presents a Bayesian kriging-based REM for coverage hole detection in outdoor urban and rural environments. In [8], a pixel-level performance assessment was done, i.e. every single uncovered pixel was considered as a coverage hole, independently of the situation of the surrounding pixels. However, N neighboring uncovered pixels do not constitute N coverage holes but a single coverage hole. Therefore, in this paper, differently form [8], we define a coverage hole as N *neighboring* uncovered pixels, and we use this definition in performance evaluations. This definition was introduced by the authors in [9], where a local coverage hole prediction is presented. In this paper, we substantially extend the solution to the cellular coverage analysis and the evaluation process, with additional scenarios and more extensive analysis of the results. To the best of our knowledge, automated coverage analysis based on spatial statistics has been studied extensively so far for sensor networks but not for cellular networks. So this paper's line of work is the first to introduce spatial statistics in cellular coverage studies and to perform realistic performance evaluations. However, the significance of this work reaches beyond: considering that MDT measurements are currently on their way to overcrowd the operator databases, operators are in need of cost effective, feasible and well-performing solutions that allow them make use of the valuable information for high quality network performance, and this paper provides a cognitive radio-inspired candidate solution. The outlined REM methodology is also potentially very efficient implementation and optimization framework for the future cognitive (self-organizing) femto cellular and HetNet systems, which will be gradually emerging as as a part of overall network architecture of cellular operators.

The rest of this paper is organized as follows. Section II presents the proposed methodology for the coverage hole detection, i.e. measurements used, the considered scenarios and developed algorithm for coverage analysis. Section III presents the REM construction method and the metrics used to represent the results. Section IV presents the performance of the proposed methodology in the automated coverage analysis. Finally, Section V summarizes our main conclusions.

II. Scenarios and methodology

The data we have used for this study consist of 3G received pilot powers, i.e. *Received Signal Code Power (RSCP)* values. The geo-located RSCP measurements are obtained with a very accurate planning tool which uses a sophisticated ray-tracing propagation model developed and used for operational network planning [10]. The propagation model uses specific environment information such as terrain profile, height, clutter, buildings etc. and is calibrated through repeated drive tests. Therefore, the RSCP data obtained from this tool and used in this work can be considered as real measurements reflecting the ground-truth on the coverage situation in the area of interest.

Considering that we are currently in the deployment phase of Long Term Evolution (LTE) technology, it is more relevant and timely to address coverage issues in LTE rather than in 3G which has been in use since nearly 10 years now. Therefore, we align our coverage detection and prediction work with LTE. For this purpose, we translate/map the RSCP measurements in 3G to their equivalent metric in LTE, namely the *Reference Signal Received Power (RSRP)*.

RSCP is the received power on the Common Pilot Channel (CPICH) measured over the 5 MHz 3G carrier bandwidth, and the RSRP is the linear average of the received powers on the time-frequency resource elements that carry cell-specific reference signals over the 15 kHz LTE carrier bandwidth. Assuming that we use the same overall bandwidth (5 MHz) for both systems, we can apply the solution presented in [11] to obtain the wideband RSRP, which is the sum of the RSRP values measured over all reference subcarriers in the bandwidth. Due to the similarity between RSRP and RSCP, authors in [11] propose to compute the wideband RSRP based on the measured RSCP values through the following equation:

$$RSRP_{5\text{ MHz}} = RSCP + 10\log\left(\frac{RS_{\text{Tx power}}}{CPICH_{\text{Tx power}}}\right) + \Delta_{pl} + \Delta_{lb} \quad (1)$$

where Δ_{pl} is the over-the-air path loss difference between the carrier frequencies of the two technologies and Δ_{lb} is the link budget difference between LTE and 3G systems. Δ_{lb} includes Node B and device antenna gains, receiver's noise figure and feeder loss differences.

In the solution presented in [11], the authors assume the usual cell planning strategy for a new technology roll-out deployment, where the existent sites are reused, antennas have the same coverage size and beamwidths, with the same antenna azimuths and tilt settings. Therefore, it is assumed that transmitter and receiver antenna gains are the same for both technologies. The extension of results given by Equation (1) to a 20 MHz LTE system is straightforward: we change the considered bias, which would imply also a change in the considered RSRP threshold.

In this paper we consider two different environments: (1) an urban area in the south west of Paris, whose received signal power map is presented in Figure 1(a), and (2) a rural area about 20 km south of Paris, whose received signal power map

is presented in Figure 1(b). In what follows we refer to these maps as the *real* coverage urban and rural maps, respectively. Both maps have a grid granularity of $25\ \mathrm{m} \times 25\ \mathrm{m}$. We refer to this grid area as a *pixel*.

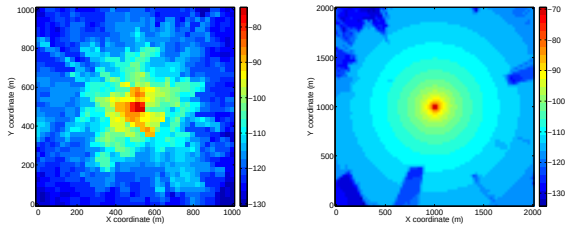

(a) Urban scenario. (b) Rural scenario.

Fig. 1. RSRP real coverage maps measured in dBm for a grid size of $25\ \mathrm{m} \times 25\ \mathrm{m}$.

Operators do not have the whole information on the ground-truth as in Figures 1. Instead, they have a partial map where they lack coverage information in some pixels. Figure 2 represents an example of such a partial coverage map that the operator could potentially have, for $p = 50\%$ of pixels with available information for the urban scenario case. In Figure 2, black pixels represent those grid areas where operator lacks the RSRP information[1]. With such a map at hand, the operators carry out detailed analysis to perform coverage detection and prediction. These analysis are performed manually by human experts, combining information coming from other sources such as alarm tickets, customer complaints etc. Needless to say, this process is long, expensive and cumbersome. To add to these drawbacks, additional drive tests may be needed in cases/areas where the available information is deemed insufficient and the coverage problem too important. What we propose instead, is to replace this manual process by an efficient automated process that uses the available measurements, avoiding or minimizing drive tests together with the expenses and delays they imply. The proposed automated process applies Bayesian kriging to the partial map of Figure 2 to obtain a REM which provides RSRP predictions in the black pixels. This automated process is managed by a software framework, called as the *REM manager*, located at the OMC. Therefore, the proposed methodology does not imply any modification in the existing network entities. This makes its deployment very straightforward and cost-effective.

We define a minimum RSRP threshold $\delta = -124$ dBm and those pixels where the received RSRP is below this threshold are considered to be out of coverage. Applying this threshold to the real coverage map we obtain a binary map of Figure 3, for the urban case, where the uncovered pixels are represented in gray, and the covered pixels are represented in white. Let $\mathcal{M}$ denote the matrix representation of the real coverage map with $\mathcal{M}(r, c)$ as the RSCP value at the r^{th} row and the c^{th} column, for $r = 1, ..., R$ and $c = 1, ..., C$. $\mathcal{P}$, with $\mathcal{P}(r, c)$ as its entry at the r^{th} row and c^{th} column, which is constructed as follows and represented in Figure 3:

- Each value in $\mathcal{M}$, $\mathcal{M}(r, c)$, where $r \in R$ and $c \in C$ is compared to δ

[1]In Figure 2, the measurement pixels are chosen randomly for reasons of simplicity. In reality, the measurement locations are expected to follow certain mobility patterns. Note that incorporation of realistic mobility patterns in measurement locations is part of the ongoing research work.

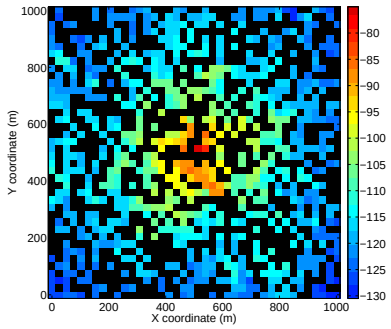

Fig. 2. RSRP measurements available for interpolation in the urban scenario.

- If $\mathcal{M}(r, c) < \delta$ we set $\mathcal{P}(r, c) = 0$
- If $\mathcal{M}(r, c) \geq \delta$ we set $\mathcal{P}(r, c) = 1$

Another important parameter to define is the minimum number of neighboring uncovered pixels which an operator considers as an area with coverage problems where some actions have to be taken. We refer to this area as a *coverage hole* and we use a typical value of $N = 4$ neighboring pixels, given the size of our grid. Two pixels are considered neighbor pixels when there is at least a common edge between them.

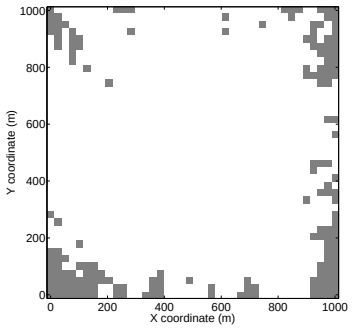

Fig. 3. Binary coverage map for δ for the urban scenario.

Algorithm 1 presents the solution we have developed to analyze the binary coverage matrix, $\mathcal{P}$, to determine the existent coverage holes. We construct a new matrix $\mathcal{N}$, where at the end all the values will be zeros, except those determined as belonging to a coverage hole.

III. REM CONSTRUCTION AND PERFORMANCE EVALUATION

The coverage analysis performed by the REM manager consists of the following steps:

1) The REM manager collects all the available RSRP measurements for the coverage analysis. In case the percentage of available measurements p is below a minimum required threshold, it can send measurement requests to the UEs over the region of interest and wait until the required minimum percentage level is reached. Here, it is worth pointing out that since we consider a semi-static scenario, time is not an issue. In any case, the delay implied by waiting for the UE measurements will always be smaller than the required time to perform drive tests.

Algorithm 1 Binary matrix analysis for coverage hole detection

```
count = 0
prev row = 0
current row = 0
𝒩 = 0
for each r do
  for each c do
    if 𝒫(r, c) = 0 then
      if 𝒫(r, c) = first CH pixel in c then
        count := count + 1;
        𝒩(r, c) = count;
      end if
      if 𝒫(r, c − 1) = 0 then
        𝒩(r, c) = 𝒩(r, c − 1)
      end if
      current row[lenght(current row + 1)] = c;
    end if
    v = intersection(current row, prev row);
    for i := 1 to v do
      l = min(𝒩(r − 1, v(i)), 𝒩(r, v(i)));
      m = max(𝒩(r − 1, v(i)), 𝒩(r, v(i)));
      (𝒩 == m) = l;
    end for
    prev row = current row;
    current row = 0;
  end for
end for
```

2) Using the available measurements, the REM manager performs the Bayesian interpolation [12] to predict the RSRP values in those pixels where it lacks measurements. A more detailed description of Bayesian interpolation for REM construction is given in [8], [13]. Finally, the REM manager constructs the REM by combining the available real measurements and the predictions.

To present the gains obtained by the REM in coverage analysis, we define the following metrics, where predicted coverage hole refers to a coverage hole detected in the REM, and real coverage hole refers to those coverage holes in the real map.

- *The average number of detected coverage holes* is the number of the real coverage holes that are correctly detected, averaged over the iterations. A coverage hole is considered as correctly detected if $c\%$ of the pixels of this coverage hole belong to a predicted coverage hole (so called in the reminder the "corresponding" real coverage hole).
- *Coverage hole detection probability* is the probability for a real coverage hole to be correctly detected, as a function of c. This probability is evaluated by dividing at each snapshot, the number of detected coverage holes by the total number of real coverage holes, and averaging the resulting ratio over the iterations.
- *Coverage hole prediction accuracy*. This metric evaluates, in average, the accuracy of the coverage hole prediction process. In other words, we evaluate to what extent the shape and the size of the detected coverage hole correspond to the reality. This metric is computed as follows: for each detected coverage hole, the number of correctly detected pixels (belonging to the corresponding real coverage hole) is divided by the total number of pixels of the corresponding real coverage hole. This ratio is then averaged over the number of real coverage holes at each iteration and over the iterations.
- *False alarm coverage hole detection* measures the number of detected coverage holes that do not correspond to any real coverage hole.

IV. Coverage hole simulation results

In order to have statistically significant results for the above metrics, their statistics are computed over 100 independent snapshots. Results presented in this section have been calculated for different percentages of available measurements, $p = \{50, 60, 70, 80, 90\}\%$ used in the interpolation process. Having $80\% - 90\%$ of measurements may seem excessive. However, when we translate p into a more tangible metric, such as the number of measurements per square meter, we obtain $q = \{0.08, 0.096, 0.112, 0.128, 0.144\}$ UE measurements per square meter, which is a small amount due to the static nature of the problem and the size of the grid.

In what follows, we evaluate the performance of the proposed coverage analysis approach. Figures 4 and 5 represent the average number of detected coverage holes for both cases, when using only network measurements and when using the REM for the urban and the rural scenarios, respectively. In both figures, the dashed black line represents the number of real coverage holes. Results presented in both figures were obtained for $c = 70\%$. As it was expected, for both cases, when the REM is used, the predicted coverage holes increase with the number of measurements used in the interpolation process, p. These figures give the notion of the average misdetection in the coverage hole detection, since the difference between the number of real coverage holes (dashed lines) and the bars are the average real coverage holes misdetected.

Specifically, for the case of the urban scenario, in Figure 4, it can be observed that in average, more than the half of the coverage holes are predicted when the REM is applied, even for the case of low amount of available measurements, $p = 50\%$. For this case, the prediction probability increases in more than 15% when the REM is applied, in comparison to the case when only measurements are used. A similar behavior can be observed for the rural scenario, presented in Figure 5, where nevertheless, statistics are less representative due to the amount of coverage holes, 5, and their size. Anyhow, when $p = 50\%$ the use of the REM increases the probability of predicting the coverage hole in 10%.

Figures 6 and 7 represent the coverage hole detection probability for $c = \{50, 70, 90\}\%$ when the REM is used. It can be observed that, when half of the coverage hole pixels are required to be detected, $c = 50\%$, the coverage hole is detected in more than 80% and 70% of the cases for urban and rural scenarios, respectively, even for low amounts of available measurements, i.e. $p = 50\%$. For the urban scenario, in Figure 6, it can be observed that for the highly demanding case of $c = 90\%$, the coverage hole is detected in more than 45% of the snapshots when p is above 70%, and the detection probability doubles for $p = 90\%$. For the rural case, as presented in Figure 7, given the fact that coverage holes are big, e.g. N bigger than 10 pixels, it is complex to achieve the highly demanding requirement of detecting $c = 90\%$ of the pixels forming the coverage hole. Nevertheless, when 90%

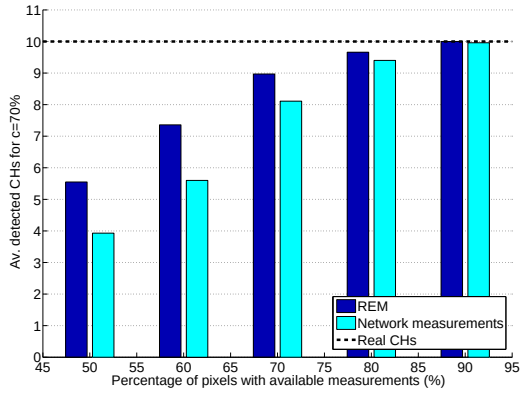

Fig. 4. Comparison of existent and predicted coverage holes with and without the REM in the urban scenario.

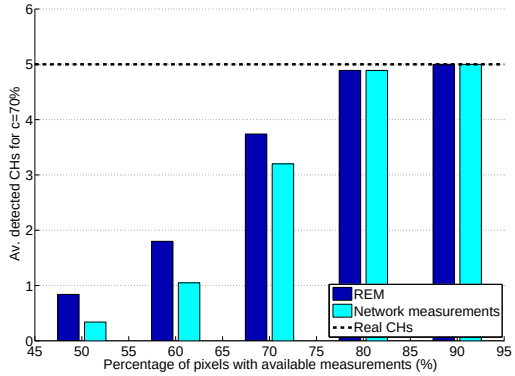

Fig. 5. Comparison of existent and predicted coverage holes with and without the REM in the rural scenario.

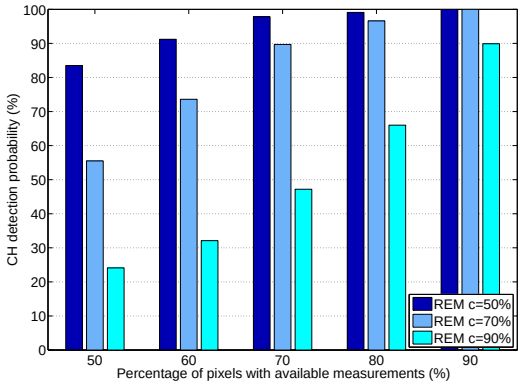

Fig. 6. Average probability of coverage hole detection for different percentages c of pixels for which measurements are available (see end of Section III), when using REM in the urban scenario.

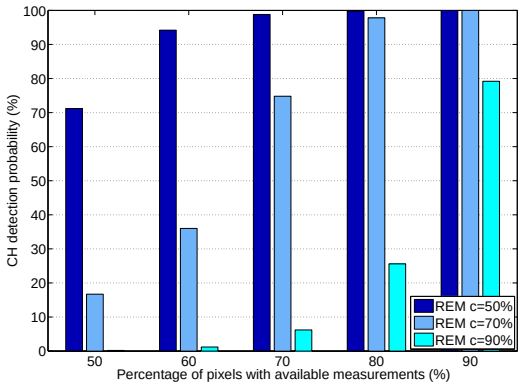

Fig. 7. Average probability of coverage hole detection for different percentages c of pixels for which measurements are available, when using REM in the rural scenario.

of measurements are available, the probability of detecting the coverage hole for $c = 90\%$ reaches a value higher than 80%.

In Figure 8, we compare the coverage hole prediction accuracy obtained for both, the urban and the rural scenarios. Dark blue bars represent results obtained for the urban scenario and light blue bars represent the results for the rural case. As the number of pixels with available measurements, p, goes higher, the probability of correctly estimate the signal power in those pixels where the operator lacks information, increases. Figure 8 shows that, in average, more than 50% of the coverage hole pixels are correctly predicted when using the REM in both scenarios, even when $p = 50\%$. The average percentage of detecting the coverage hole pixels is higher than 90% when $p = 90\%$.

Finally, Figure 9 represents the average number of false alarm coverage holes predicted by the REM for both, the urban and the rural scenarios. The dark and light blue dashed lines represent the real coverage holes in the real map for the urban and rural cases, respectively. Specifically, the rural scenario presents a large amount of false alarm coverage holes when the available measurements are low ($p = 50\%$) because the interpolation process is not able to correctly integrate in its prediction model the effects of deep shadowing barriers, as it is the case in the (bottom part of the rural scenario, Figure 1(b)). Nevertheless, as the amount of measurements increases, the false alarm probability notably decreases as well, reaching a close to zero value when $p = 90\%$. For the urban case, the average false alarm coverage holes detected are low, around 3, even for $p = 50\%$.

On the overall, we observe that the gains brought by the proposed approach (with respect to the "measurements only" case) are higher with the decreasing percentage of available measurements. This proves that the proposed approach fulfills its purpose of providing a cost-efficient solution without a compromise on the performance. Its detection performance gets significantly better if we relax the minimum requirements for coverage detection (small values of c) but even in that case, the prediction accuracy is high enough to guarantee an overall high-quality detection and prediction performance. Comparing the rural and urban cases, we observe that coverage hole detection performs better for cases where the coverage holes are small in size and large in number (typical urban environment) compared to the opposite case where the coverage holes are small in number and large in size (typical rural environment). As for coverage hole prediction, the quality is high in both cases. A possible solution for rural coverage hole detection is then to adopt a *multi-resolution* approach: carry out a high-level global coverage detection with low granularity at first (as

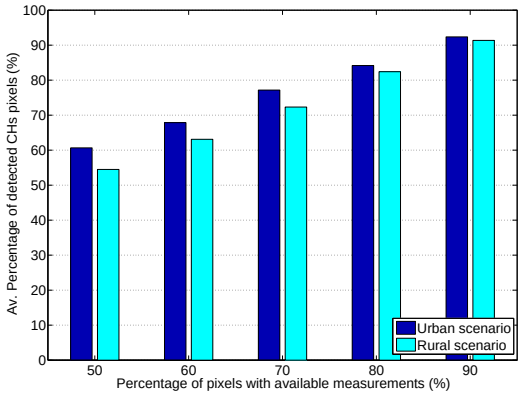

Fig. 8. Prediction accuracy with REM for the urban and rural scenarios.

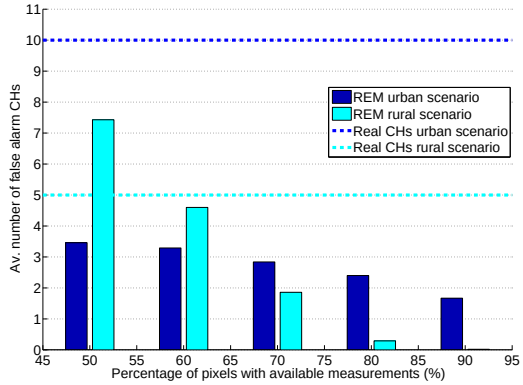

Fig. 9. Probability of false alarm in the coverage hole detection when using REM for the urban and rural scenarios.

described in this paper), followed by a local analysis with high granularity on those regions that need further precision. The multi-resolution approach constitutes one of the main further research areas in this line of work.

V. Conclusions

In this work we presented a remote and automated solution for coverage detection and prediction for cellular networks. Our approach is firmly based on cognitive radio techniques, and shows how methods developed for adaptive future wireless networks can bring significant benefits also to the management of the present-day wireless systems. We studied the performance gains introduced by the use of REMs in the automated coverage analysis problem. REM is built by applying powerful spatial interpolation techniques (Bayesian kriging) to the available measurements, and it is used to detect those areas with potential coverage problems and predict the shape of those areas. The proposed automated solution replaces the long and expensive task of manual coverage hole analysis and it allows the operators to rapidly deploy solutions which overcome the coverage problem. The obtained results demonstrate that the REM-based automated coverage detection and prediction is a promising approach for future cognitive cellular networks, which is worth further studies/investigations.

As future work, we have two main lines of research, on the one hand, we want to introduce, in the evaluation process, the density of population patterns as well as the measurements accuracy in terms of location. On the other hand, we see the application of multi-resolution REMs for the coverage hole detection problem as an interesting possibility we would like to explore.

Acknowledgment

The authors would like to thank Jean-Baptiste Landre, from Orange Labs, for his helpful comments. We thank EU for providing partial funding of this work through the FARAMIR project (grant number ICT-248351). JR and PM also thank RWTH Aachen University and DFG for partial financial support through the UMIC research centre.

References

[1] "3GPP TR 36.805 v1.3.0 1 study on minimization of drive-tests in next generation networks; (release 9)," 3GPP organization, Tech. Rep., Nov. 2009.

[2] H. Holma and A. Toskala, *LTE Advanced: 3GPP Solution for IMT-Advanced*. John Wiley & Sons.

[3] J. Mitola, *Cognitive radio: an integrated agent architecture for software defined radio*. (Doctoral dissertation), Royal Inst. Technol.(KTH), Stockholm, Sweden, 2000.

[4] Y. Zhao, B. Le, and J. H. Reed, "Network support - the radio environment map," in *Cognitive Radio Technology*, B. A. Fette, Ed. Elsevier, ch. 11.

[5] A. Alaya-Feki, B. Sayrac, S. Ben Jemaa, and E. Moulines, "Interference cartography for hierarchical dynamic spectrum access," in *New Frontiers in Dynamic Spectrum Access Networks, 2008. DySPAN 2008. 3rd IEEE Symposium on*, Oct. 2008.

[6] A. Alaya-Feki, S. Ben Jemaa, B. Sayrac, P. Houze, and E. Moulines, "Informed spectrum usage in cognitive radio networks: Interference cartography," in *Personal, Indoor and Mobile Radio Communications, 2008. PIMRC 2008. IEEE 19th International Symposium on*, Sept. 2008.

[7] J. Riihijärvi, P. Mähönen, M. Wellens, and M. Gordziel, "Characterization and modelling of spectrum for dynamic spectrum access with spatial statistics and random fields," in *Personal, Indoor and Mobile Radio Communications, 2008. PIMRC 2008. IEEE 19th International Symposium on*, Sept. 2008.

[8] B. Sayrac, J. Riihijärvi, P. Mähönen, S. Ben Jemaa, E. Moulines, and S. Grimoud, "Improving coverage estimation for cellular networks with spatial bayesian prediction based on measurements," in *Proceedings of the 2012 ACM SIGCOMM workshop on Cellular networks: operations, challenges, and future design*, ser. CellNet '12, 2012, pp. 43–48.

[9] A. Galindo-Serrano, B. Sayrac, S. Ben Jemaa, J. Riihijärvi, and P. Mähönen, "Automated coverage hole detection for cellular networks using radio environment maps," in *The 9th International Workshop on Wireless Network Measurement (WiNMee 2013), in conjuction with WiOPT 2013.*, May 2013.

[10] ASSET, Website, http://www.aircominternational.com/Products/planning/asset.aspx.

[11] J.-B. Landre, Z. E. Rawas, R. Visoz, and S. Bouguermouh, "Realistic performance of LTE: In a macro-cell environment," in *Vehicular Technology Conference (VTC Spring), 2012 IEEE 75th*, May 2012.

[12] H. Omre, "Bayesian kriging–merging observations and qualified guesses in kriging," *Mathematical Geology*, vol. 19, no. 1, pp. 25–39, January 1987.

[13] S. Grimoud, B. Sayrac, S. Ben Jemaa, and E. Moulines, "Best sensor selection for an iterative REM construction," in *Vehicular Technology Conference (VTC Fall), 2011 IEEE*, Sept. 2011.